

# Dynamical studies and product analysis of O(<sup>1</sup>D) + H<sub>2</sub>/D<sub>2</sub> reactions

CAROLINA M. A. RIO and JOAO BRANDAO\*

Dept. Química, Bioquímica e Farmácia—FCT, Universidade do Algarve,  
Campus de Gambelas, 8005-139 Faro, Portugal

(Received 28 November 2006; in final form 6 December 2006)

The aim of this study was to analyse the dynamics of O(<sup>1</sup>D) + H<sub>2</sub>/D<sub>2</sub> reactions using quasiclassical trajectory calculations on a double-valued potential energy surface for H<sub>2</sub>O. Produced on the photodissociation of stratospheric ozone, the excited oxygen atom is a highly reactive species whose chemistry plays a key role in the ozone depletion cycle. In order to make comparisons with experiment, we studied these reactions at fixed translational collision energies. In particular, we consider the reactive cross sections, the thermal rate constants, the opacity function, and the differential cross sections. In addition, we also study the energy distribution of the products and compare the results with experiment and calculations based on phase space statistical theory. Results for the rotational population of the OH products are also compared with experimental results. The agreement between our results and experiment reinforces the accuracy of the H<sub>2</sub>O potential energy surface used.

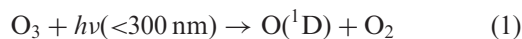
*Keywords:* Molecular dynamics; Atmospheric chemistry; Chemical kinetics

## 1. Introduction

Due to its important role in atmospheric chemistry, the reaction O(<sup>1</sup>D) + H<sub>2</sub> → OH + H and its isotopic variants have been the subject of various experimental studies [1–8]. Numerous theoretical studies of its dynamics have also been carried out (for example, see [1, 5–7, 9–20]) using the potential energy surfaces (PES) published for this system [9, 21–32].

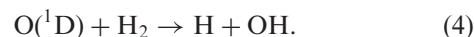
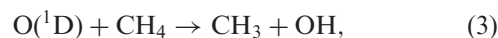
In the stratospheric ozone layer, located at an altitude of between 13 and 50 km, the absorption of radiation at wavelengths of between 200 and 300 nm (the Hartley band) (see equation (1)) is of fundamental importance for the reduction of photons of wavelength of less than 300 nm which cause biological mutation, solar burning and other physiological effects [33]. The decrease of the ozone layer is a well-known problem (see, for example, [34–37]).

The excited oxygen atom produced by the reaction



is a very reactive species that quickly attacks methane, water vapour and molecular hydrogen present in the

stratosphere [38], producing hydroxyl radicals according to the reactions



These OH radicals initiate a slow and two rapid catalytic HO<sub>x</sub> cycles of destruction of the stratospheric ozone, which can eliminate about 10% of the existing ozone [39].

At room temperature the reactivity of O(<sup>1</sup>D) with the hydrogen molecule is about seven orders of magnitude higher than that of the ground state oxygen atom, O(<sup>3</sup>P); the uncertainty in the accuracy of this parameter is an important source of error in ozone depletion studies.

Five potential energy surfaces are accessible to the reactants, but the main contribution comes from the lowest (<sup>1</sup>A') PES, which correlates with the (<sup>1</sup>A<sub>1</sub>) ground state of the H<sub>2</sub>O molecule. The first excited state, <sup>1</sup>A'', must be considered for energies higher than 8.4 kJ mol<sup>-1</sup> [13]; this contribution being approximately 0.3 × 10<sup>-10</sup> cm<sup>3</sup> molecule<sup>-1</sup> S<sup>-1</sup> for a temperature of 1000 K. In addition, Hsu *et al.* [8] estimated a constant contribution of approximately 10% from the <sup>1</sup>Π state at collinear geometries, due to the non-adiabatic

\*Corresponding author. Email: jbrandao@ualg.pt

electrostatic coupling between the  $^1\Sigma^+$  ( $1^1A'$ ) and  $^1\Pi$  ( $2^1A'$  and  $1^1A''$ ) states.

It has been stated that, on the ground state surface, this reaction proceeds via an insertion mechanism followed by a vibrationally excited water molecule. Using the potential energy surfaces of Murrell *et al.* [26] (MC PES), Schinke and Lester [28] (SL PES) and Ho *et al.* [17] (K or RKHS PES), Schatz *et al.* [40] report that the average scattering angle is close to 1.57 rad ( $90^\circ$ ). This is verified when several rotational periods occur before dissociation of the complex into products, but this symmetric angular distribution can also arise from collisions proceeding via insertion [41]. On the other hand, this reaction is believed to occur through an abstraction mechanism on the first excited surface [7, 8].

We have published a double-valued potential energy surface for the ground-state water molecule,  $^1A'$ , henceforth referred to as Brandão and Rio [21] (BR PES), that includes a careful description of the long-range interactions as described in [11], which should play an important role in the dynamics of this barrierless reaction. The double-value form of this BR PES allows us to describe, on the lower adiabatic surface, the crossings between different diabatic surfaces and correctly represent all the dissociation channels of the ground-state water molecule. To calibrate this surface we have used accurate *ab initio* results [42] complemented with published data [43, 44].

Using this BR PES, the computed thermal rate constants for the title reaction proved to be in very good agreement with experimental values, using either quasiclassical trajectories (QCT) [45] or quantum mechanical (QM) calculations [46]. Also on the same BR PES, the quasiclassical trajectory calculations carried out for the isotopic exchange reaction  $D + OH \rightarrow H + OD$  by Wang *et al.* [47] were shown to be in good agreement with experimental results, corroborating the representation of the intersection of singlet surfaces that occurs in this potential.

In addition, there is a large amount of experimental information on the title reaction at fixed translational energies, focusing on the differential cross sections and product energy distributions, which should be compared with theoretical predictions using this BR PES to confirm its quality.

Experimentally, Alagia *et al.* [2] studied the reaction  $O(^1D) + H_2$  at collision energies of 8.0 and 12.6 kJ mol $^{-1}$ , and the reaction  $O(^1D) + D_2$  at 22.2 kJ mol $^{-1}$ . Ahmed *et al.* [1] also studied the latter reaction at a collision energy of 10.0 kJ mol $^{-1}$ .

Aoiz *et al.* [3–5] presented an experimental study of the distribution of the rotational population of the products of the reaction  $O(^1D) + H_2$ . They compared the distributions for rotational quantum states of the OH

product with QCT and QM calculations for the  $1^1A'$  and  $1^1A''$  surfaces. QCT and QM calculations have been carried out both for the K surface [17] and the DK PES [22, 48]. The results of Aoiz *et al.* [5] at 5.4 kJ mol $^{-1}$  (56 meV) suggest that the  $1^1A''$  PES does not contribute to the reaction at this energy, which is particularly useful for making a comparison with our results.

Using this new potential energy surface  $^1A'$  BR PES we performed quasiclassical trajectory studies [49, 50] for the  $O(^1D) + H_2$  and  $O(^1D) + D_2$  reactions at the above collision energies and compared the results with the experimental data and results for previous potentials. See [45] for computational details.

This article is organized as follows. In section 2, we analyse the reactive cross sections, the thermal rate constants and the opacity function for  $O(^1D) + H_2/D_2$  reactions. Section 3 describes the differential cross sections or angular distributions of the products. In section 4 we study the energy distribution of the products and make a comparison with experiment and statistical estimations. The distribution of the rotational and vibrational populations is also analysed for the  $O(^1D) + H_2$  reaction in this section. Section 5 reports the conclusions.

## 2. Reactive cross section and thermal rate constants

We carried out calculations at fixed translational collision energies of 2.1, 4.2, 5.4, 8.0, 12.6 and 20.9 kJ mol $^{-1}$  for the reaction  $O(^1D) + H_2$ . For the 8.0 and 12.6 kJ mol $^{-1}$  calculations, we used the diatomic initial conditions reported in [2]; otherwise, we used the Boltzmann distribution at 300 K for the vibrational and rotational energies of the  $H_2$  diatomic. Additional values of 2.1, 4.2 and 20.9 kJ mol $^{-1}$  were chosen in order to study the general trend of the reactive cross sections.

Table 1 summarizes the trajectory details (maximum impact parameter, number of computed and reactive trajectories) and the resulting cross sections. We can see that the reactive cross section decreases with increasing collision energy, as expected for reactions that proceed without a barrier and are dominated by long-range forces. Recently, Lin and Guo [46] computed quantum integral cross sections for the  $O(^1D) + H_2$  reaction using the same BR PES; a comparison of these quantum results and our QCT results is shown in figure 1. The agreement is good and validates the use of classical mechanics in these studies. Also in this figure we show the QCT results using the K PES [51] and the trajectory results on the DK PES [16].

These reactive cross sections can be considered as the sum of a capture term, which decreases with energy, and

a rigid sphere term, which is constant and should dominate at high energies. Using the expression

$$\sigma(E) = \sigma_{\text{cap}}(E) + \sigma_{\text{rs}} = AE^{-m} + B, \quad (5)$$

we were able to estimate the thermal rate constants for this reaction,

$$k(T) = g \left( \frac{2}{k_B T} \right)^{3/2} \left( \frac{1}{\pi \mu} \right)^{1/2} \int_0^\infty E \sigma(E) e^{-E/(k_B T)} dE \\ = \frac{1}{5} \left( \frac{8k_B T}{\pi \mu} \right)^{1/2} \left[ A \frac{\Gamma(2-m)}{(k_B T)^m} + B \right], \quad (6)$$

where  $k_B$  is Boltzmann's constant,  $\mu$  is the reduced mass of  $O + H_2$  and  $A = 2.239 \times 10^{-27}$ ,  $m = 0.6787$  and  $B = 1.237 \times 10^{-13}$ . The units of these parameters are such that the rate constant will be in  $\text{cm}^3 \text{molecule}^{-1} \text{s}^{-1}$  when using SI values for the constants. The value of

$1/5$  for  $g$  accounts for the electronic degeneracy as we consider only one of the five PESs accessible to the reactants.

In figure 2, we compare the results obtained using equation (6) with experimental estimates for the  $O(^1D) + H_2$  reaction. We also present the quantum results [46] and previous QCT thermal rate constant results [45], both using the same BR PES. Different from the present calculations, in our earlier work we randomly generated the translational collision energy as well as the diatomic internal rotational and vibrational energies according to the Boltzmann distribution at each temperature. Both QCT results agree for temperatures above 150 and predict a constant value for  $k(T)$  at lower temperatures. The differences at low temperatures can be attributed to imprecision in the fitting of the cross sections at low energies and to discrepancies in the description of the internal energy of the diatomic. The QM results [46] agree with the QCT results at temperatures above 300 K but, in contrast, they exhibit very distinct behaviour at lower temperatures. The latter authors claim that this difference is an indication of the quantum effects due to resonances near the threshold and to the lack of re-crossing effects in the classical treatment. We also note that their results are not averaged over the possible internal states of the diatomic reactant.

As stated above when characterizing this reaction, two additional contributions should be taken into account before comparison with experiment. When they are considered, Brandão and Rio [45] obtained rate constants in close agreement with experiment,

Table 1. Reactive cross section and mean lifetime of the complex for the reaction  $O(^1D) + H_2$ .

$E_{\text{col}}$ (kJ mol <sup>-1</sup> )	$b_{\text{max}}$ (Å)	$N_T$	$N_R$	$P_R$	$\sigma_r \pm \sigma_{\text{or}}$ (Å <sup>2</sup> )	$\langle t_{\text{cl}} \rangle$ (fs)
2.1	4.0	9999	5887	0.589	29.59 ± 0.25	81.9
4.2	3.8	10,000	5022	0.502	22.78 ± 0.23	83.3
5.4	3.0	20,000	15,421	0.771	21.80 ± 0.08	87.4
8.0	3.0	10,000	6791	0.679	19.20 ± 0.13	87.7
12.6	2.8	10,001	7075	0.707	17.42 ± 0.11	90.3
20.9	2.5	10,001	8151	0.815	15.99 ± 0.08	92.8

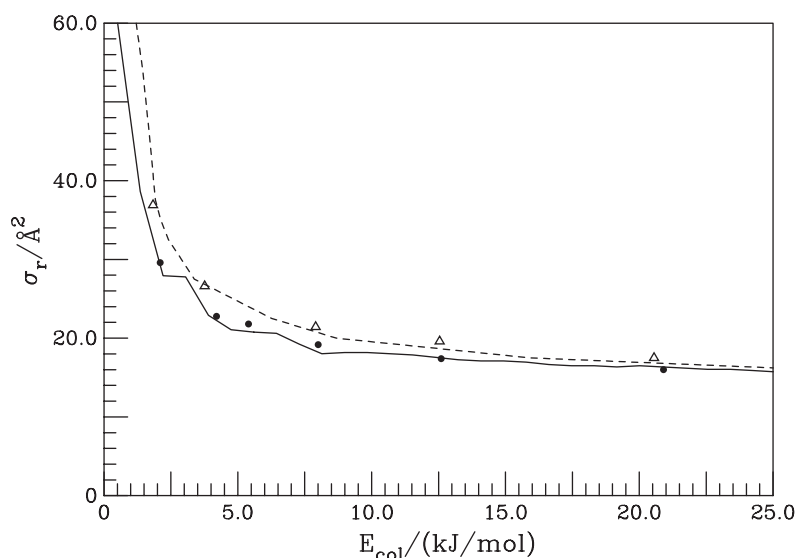


Figure 1. Reactive cross section as a function of the collision energy for the reaction  $O(^1D) + H_2$ . (●) QCT results, this work. (—) QM results using the BR PES [46]. (- - -) QCT results using the K PES [51]. (△) QCT results using the DK PES [16].

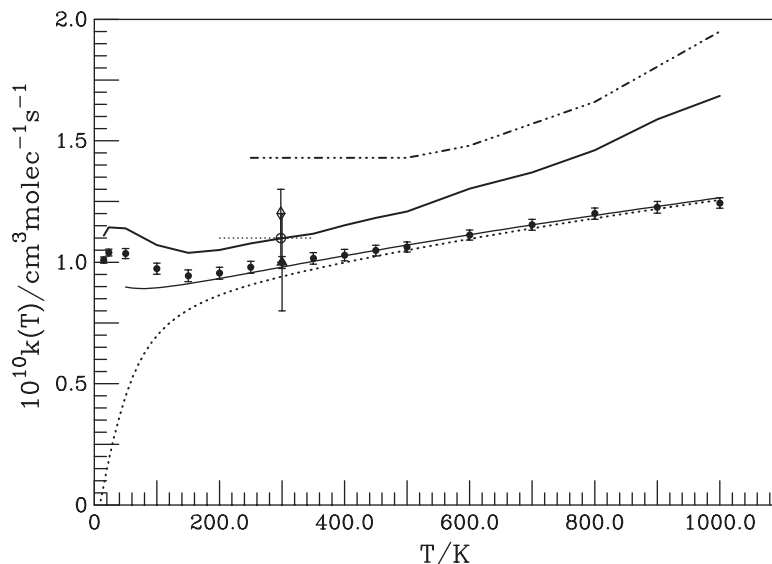


Figure 2. Rate constants for the reaction  $\text{O}(^1\text{D}) + \text{H}_2$ . (—) Equation (6), previous QCT thermal results [45] ( $\bullet$ ) without correction and (---) with correction; see text) and ( $\cdots$ ) QM calculations [46], all using the BR PES. Experimental data: ( $\diamond$ ) [52]; ( $\Delta$ ) [36]; ( $\odot$ ;  $\cdots$ ) [53]. (- $\cdots$ -) QCT results [40] on the K PES considering corrections.

as shown in figure 2. We also present the QCT results obtained using the K surface [40] considering the contributions of the excited surfaces. The greater reactivity found for the K PES is in accordance with the larger cross sections exhibited by this PES, as shown in figure 1.

The average values of the complex lifetime are reported in the last column of table 1. We considered as complexes the configurations where the potential energy assumes a value of  $0.2 \text{ eV}$  ( $19.2 \text{ kJ mol}^{-1}$ ) below the  $\text{H} + \text{OH}$  dissociation energy and the complex lifetime was considered to be the time elapsed between the first entrance of a trajectory in this potential region and its last exit. We observe that the average lifetime of the formed complex increases slightly with increasing collision energy. This unexpected result seems to be consistent and can be attributed to an increase in the centrifugal barrier to dissociation.

When considering the  $\text{O}(^1\text{D}) + \text{D}_2$  reaction, we computed quasiclassical trajectories at  $10.0$  and  $22.2 \text{ kJ mol}^{-1}$  collision energy, which are the experimental energies used by Ahmed *et al.* [1], and Alagia *et al.* [2], respectively. We used the experimental internal energy distribution of the diatomic,  $5 \text{ K}$  in [1], and the quoted values reported in [2]. Similarly to the  $\text{O}(^1\text{D}) + \text{H}_2$  study, we also performed QCT calculations for the three fixed collision energies of  $2.1$ ,  $4.2$  and  $20.9 \text{ kJ mol}^{-1}$ .

The computed total reactive cross sections,  $\sigma_r$ , are reported in table 2. As for the  $\text{O}(^1\text{D}) + \text{H}_2$  reaction, the value of  $\sigma_r$  decreases with increasing collision energy.

Table 2. Reactive cross section and mean lifetime of the complex for the reaction  $\text{O}(^1\text{D}) + \text{D}_2$ .

$E_{\text{col}}$ ( $\text{kJ mol}^{-1}$ )	$b_{\text{max}}$ ( $\text{\AA}$ )	$N_{\text{T}}$	$N_{\text{R}}$	$P_{\text{R}}$	$\sigma_r \pm \sigma_{\text{err}}$ ( $\text{\AA}^2$ )	$\langle t_{\text{cl}} \rangle$ (fs)
2.1	4.0	9998	6074	0.608	$30.54 \pm 0.25$	117.8
4.2	3.8	10,000	5136	0.514	$23.30 \pm 0.23$	122.5
10.0	2.8	10,000	7388	0.739	$18.20 \pm 0.11$	136.4
20.9	2.5	10,000	8144	0.814	$15.99 \pm 0.08$	139.6
22.2	2.5	10,001	8062	0.806	$15.83 \pm 0.08$	134.7

This is shown better in figure 3, which presents the reactive cross section of both reactions as a function of the collision energy. We also display in this figure the QCT results for the  $\text{O}(^1\text{D}) + \text{D}_2$  reaction computed by Aoiz *et al.* [10] and Balucani *et al.* [6] using the DK PES, which lie above the BR PES results as for the reaction with hydrogen.

Hsu *et al.* [54] published relative experimental values for the total reactive cross section as a function of the total energy defined as the sum of the translational energy of the reagents and the small rotational energy of the target molecule. Their results are similar to ours for energies below  $8.4 \text{ kJ mol}^{-1}$ , showing a negative slope for the excitation function, where the cross section of the deuterated reaction is slightly higher than for the hydrogenated reaction. For higher total energies they showed that the first excited PES should contribute through an abstraction mechanism with different effects on the two reactions.

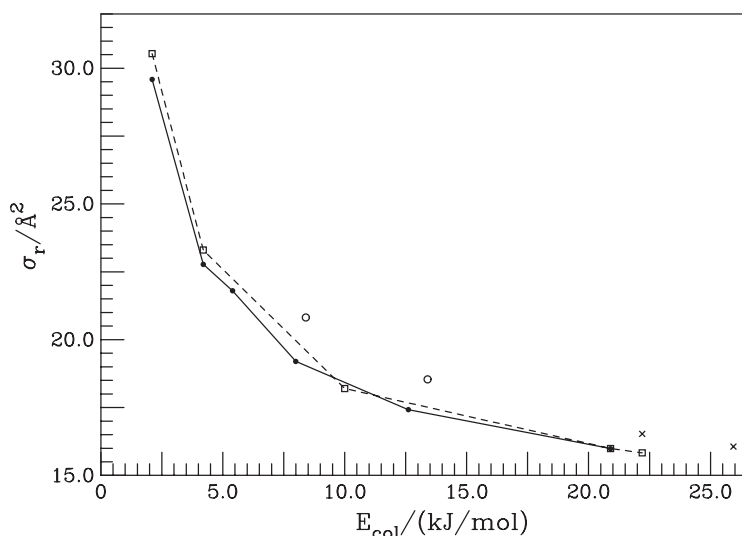


Figure 3. Reactive cross sections as a function of the collision energy. This work: (●; —) reaction  $O(^1D) + H_2$ ; (□; ---) reaction  $O(^1D) + D_2$ . QCT results for the  $O(^1D) + D_2$  reaction on the DK PES: (○) [10]; (×) [6].

In the last column of table 2 we report the average lifetime of the complex. We can see that, similar to the reaction with  $H_2$ , the average lifetime of the formed  $D_2O^*$  complex increases with increasing collision energy, but it is longer when considering the deuterated reaction. The somewhat smaller value obtained for the  $22.2 \text{ kJ mol}^{-1}$  collision energy can be attributed to the very low internal energy of the diatomic. The longer complex lifetime of deuterated water can be explained by the larger mass of the reactants and, consequently, the lower velocity. The ratio of the complex lifetime for these two reactions is 1.44, 1.47 and 1.50 at 2.1, 4.2 and  $20.9 \text{ kJ mol}^{-1}$ , respectively, which is close to the value of  $\sqrt{2}$  expected from the ratio of their reduced masses. This effect may be of importance in conditions where deactivation by collision can occur.

Another view of the dynamics of this reaction is the opacity function, defined as the probability,  $P_r(b)$ , of one trajectory being reactive at a given impact parameter,  $b$ . The opacity function for the reaction  $O(^1D) + H_2$  at several calculated collision energies presents a similar form. The reaction probability is close to 0.9 for all energy collisions at impact parameters less than  $2.2 \text{ \AA}$ , vanishing quickly for larger impact parameters. This is the behaviour we expect for a reaction that proceeds without an energy barrier. Accurate QM results for the ground DK PES [55] at a collision energy of  $9.6 \text{ kJ mol}^{-1}$  plotted by Rackham *et al.* [56] display a similar trend, but they are larger than our results at  $8.0 \text{ kJ mol}^{-1}$ , which is consistent with the greater reactivity of the DK PES. The deuterated reaction presents similar behaviour.

It is relevant to emphasize that the decay of the opacity function depends on the collision energy.

For low energies we still have a reaction for distances as large as  $3.5 \text{ \AA}$ . This clearly shows the importance of the long-range part of the potential in the dynamics of these reactions. The relationship between the collision energy and the maximum impact parameter is independent of the isotope used, as can be observed from the  $b_{\text{max}}$  values quoted in tables 1 and 2.

### 3. Differential cross section

The differential cross section or angular distribution of the products,  $d\sigma/d(\cos\theta)$ , represents the reactive cross section vs. the scattering angle,  $\theta_{\text{scatt}}$ . Being sensitive to the details of the potential energy surface used in the calculations, this constitutes one of the most important functions for understanding the dynamics of a reaction. The differential cross section is defined by the expression

$$\frac{d\sigma}{d(\cos\theta)} = \frac{NR(\theta_{\text{scatt}})}{N_T} \pi b_{\text{max}}^2 \frac{1}{2\pi \sin\theta_{\text{scatt}}}, \quad (7)$$

where  $N_R(\theta_{\text{scatt}})$  represents the number of reactive trajectories scattered at angle  $\theta$  and  $N_T$  is the total number of computed trajectories. The scattering angle of a given collision is defined as the angle between the relative velocity vector of the products  $\mathbf{v}_P$  and the relative velocity vector of the reactants  $\mathbf{v}_R$  and is given by

$$\cos\theta_{\text{scatt}} = \frac{\mathbf{v}_P \cdot \mathbf{v}_R}{|\mathbf{v}_P| \cdot |\mathbf{v}_R|}. \quad (8)$$

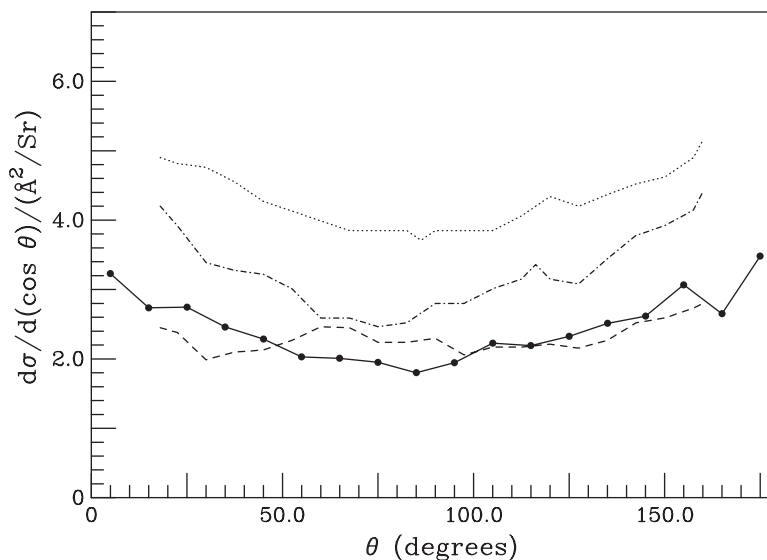


Figure 4. Differential cross sections for the reaction  $\text{O}(^1\text{D}) + \text{H}_2$  at  $2.1 \text{ kJ mol}^{-1}$  collision energy. ( $\bullet$ ; —) this work (BR PES) [21]. (---) MC PES [57]. (- · - · -) SL PES [28]. (····) K PES [17].

Analysis of the differential cross section gives, in a qualitative way, the lifetime of the complex and reflects the insertion or abstraction mechanism of the reaction.

Figure 4 compares the product angular distribution for the reaction  $\text{O}(^1\text{D}) + \text{H}_2$  at a translational collision energy of  $2.1 \text{ kJ mol}^{-1}$  with similar calculations using the potential energy surfaces MC [57], SL [28] and K [17] taken from the work of Ho *et al.* [17]. Note that the differential cross sections estimated from the MC and K potential energy surfaces have larger values, which reflects the greater reactivity predicted by these surfaces.

All these angular distributions are symmetrical, which indicates a possible long-lived complex with several rotational periods before dissociation into products. It has been reported that this result can also be obtained with direct reactions that occur through an insertion mechanism [12]. Detailed observation of our trajectories shows that this reaction proceeds via insertion through a highly excited bending mode of the complex. Using an average value for the angular momentum of the reactive collisions, we estimate that, during the mean complex lifetime, the  $\text{H}_2\text{O}$  (or  $\text{D}_2\text{O}$ ) complex has a lifetime of between 0.8 and 2.5 rotational periods depending on the orientation of the angular momentum vector, which allows us to consider it as long lived. All these factors justify the observed outcome.

The same forward-backward symmetry occurs at higher collision energies when we analyse the angular distribution of the products for the five energies studied. This result is in agreement with increasing complex lifetime with increasing collision energy, as already noted from tables 1 and 2. From these results we

conclude that the reaction mechanism, in this BR surface, is similar for all energies in this range. We also observe that the differential cross sections decrease with increasing collision energy, in accordance with the results for the total reactive cross section shown in table 1 and figure 3.

In figure 5 we compare our results with experimental data [2] for the reaction  $\text{O}(^1\text{D}) + \text{H}_2$  at collision energies of  $8.0$  and  $12.6 \text{ kJ mol}^{-1}$ . The agreement is good, in particular for the low-energy results. However, the experimental data at higher collision energy exhibit forward-backward asymmetry, which can be attributed to the contribution of the first excited state at this energy [40], not considered in this study.

A somewhat different experimental result, exhibiting small angular asymmetry, was obtained at a collision energy of  $5.4 \text{ kJ mol}^{-1}$  [5], where the contribution of the excited states should be neglected. In figure 6 we compare our results using the BR PES with the experimental measurements [5]. We also plot the QM [55] and QCT [5] calculations on the  $1^1\text{A}'$  DK PES. Due to the symmetry of our results, the agreement with experiment is not so good. In contrast, the DK PES presents higher asymmetry than experiment, but, peculiarly, in the opposite direction when considering the QCT or QM results.

Similarly, we can compare our results for the reaction  $\text{O}(^1\text{D}) + \text{D}_2$  with the experimental angular distribution of the products at collision energies of  $10.0 \text{ kJ mol}^{-1}$  [1] and  $22.2 \text{ kJ mol}^{-1}$  [2]. In figure 7, where we also plot the QCT differential cross sections computed on the  $1^1\text{A}'$  DK PES at  $22.2 \text{ kJ mol}^{-1}$  [6], good agreement is observed between our calculated results and experiment,

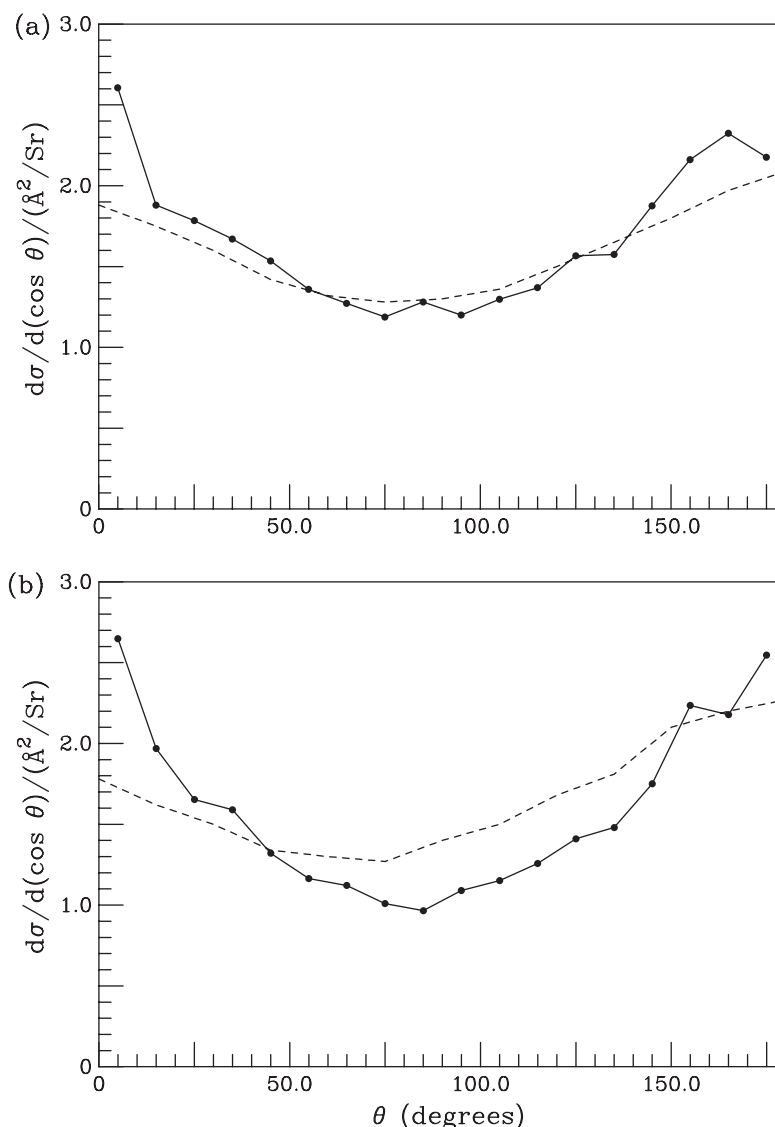


Figure 5. Differential cross sections for the reaction  $O(^1D) + H_2$  at collision energies of (a) 8.0 and (b) 12.6 kJ mol<sup>-1</sup>. (●; —) Present work. (- -) Experimental results [2].

and, again, a higher asymmetry for the DK PES results can be observed.

#### 4. Energy distribution of the products

As stated above, the title reaction proceeds via a long-lived complex prior to dissociation into products. This is a necessary condition for observation of the statistical distribution of the energy, which should be independent of the details of the PES. To test this approach, we performed statistical calculations for the  $O + H_2$  reaction, reproducing the same initial conditions used in the quasiclassical trajectory studies presented above. Using the phase space theory of Pechukas *et al.* [58], the

statistical distributions are calculated considering equally probable all product and reactant states, compatible with the total energy and angular momentum of the reactants. To avoid the details of the PES, we used isotropic entrance and exit channels built from the angular average of the leading long-range term and took into account the exothermicity of the reaction.

In table 3, we report the partition of the final total kinetic energy into its components (translational, vibrational and rotational energies) at the five fixed collision energies used in this study of the  $O(^1D) + H_2$  reaction. Table 4 displays an analogous partition for the deuterated reaction. The tables show a similar pattern of energy distribution for both reactions, close to 30% for the translational energy and close to 35% for the

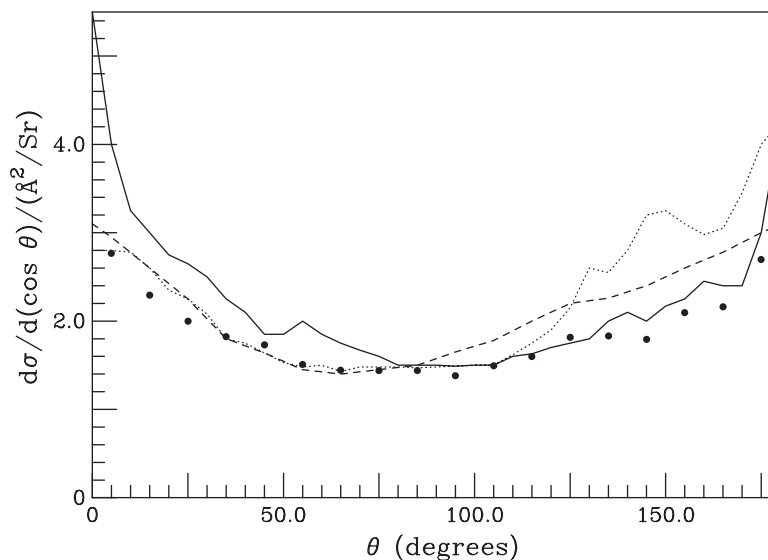


Figure 6. Angular distribution of the products for the reaction  $\text{O}(^1\text{D}) + \text{H}_2$  at a collision energy of  $5.4 \text{ kJ mol}^{-1}$ . (—) QM results on the DK PES [55]. (····) QCT results [5] on the same PES. (---) Experimental results [5]. (●) This work.

vibrational and rotational energies. The quoted results compare well with the experimental results [2] of 31.6 and 28.4% for the translational energy fraction of the  $\text{O} + \text{H}_2$  reaction at collision energies of 8.0 and  $12.6 \text{ kJ mol}^{-1}$ , respectively, and 29% for the  $\text{O} + \text{D}_2$  reaction at a collision energy of  $22.2 \text{ kJ mol}^{-1}$ . For comparison we note that, for the latter collision energy, the QCT result on the DK  $1^1\text{A}'$  PES is 32% in [6].

In contrast, the predicted statistical distribution presented in table 5 is between 37 and 40% for the translational and vibrational energies and from 22 to 25% for the rotational energy. This clearly shows that the trajectory calculations discriminate between the different energy modes in favour of a higher rotational energy of the diatomic to the detriment of the translational energy. This effect has already been noted [12] and may be a result of the dissociation of a  $\text{H}_2\text{O}$  complex highly excited on the vibrational bending mode as a result of the insertion mechanism.

This may also be due to the details of the PES on the exit channel, where the description of the intersection of the two singlet surfaces can be relevant in spite of the large exothermicity of this reaction. The long-range interactions can also play an important role in the vibrational and rotational anisotropies of the OH product [56]. As noted previously, recent results, using the BR PES to calculate the thermal rate constants of the exchange reaction  $\text{D} + \text{OH} \rightarrow \text{OD} + \text{H}$  [47], which should be sensitive to the details of this region, proved to be in very good agreement with experiment.

A different statistical result [59] has been obtained using a more detailed statistical theory of atom–diatom insertion reactions. Using the coupled-channel statistical

theory and the DK PES these authors found the distribution of vibrational levels to be close to our result, but their rotational distribution was in close agreement with accurate quantum calculations on the same PES. This may show that the details of the PES should be considered in statistical calculations.

In figure 8 we present the distribution of the translational energy of the products for some of those calculations. We also present a Maxwell–Boltzmann distribution obtained for a coarse fit of the temperature to those results. The agreement between both distributions is reasonable. We also plot the available experimental distribution and the respective error bars for the energies considered here [2]. In all cases the agreement seems reasonable when considering the experimental uncertainties in the high-energy region and the absence of the contributions due to the upper PESs. In this figure we also present the distribution predicted by statistical theory for the  $\text{H}_2$  reaction. As referred to above, the statistical results favour products with higher translational energies.

Observe that figures 8(a) and (c) refer to reactions with different isotopes but similar total energy. The final translational temperature appears to be equal and independent of the isotope. This result should be compatible with a reaction where the total energy is statistically distributed between the different modes. This differs from the result of Hsu *et al.* and Aoiz *et al.* [7, 60] for the reaction of  $\text{O}(^1\text{D})$  with HD at  $8.6 \text{ kJ mol}^{-1}$ , where a break in symmetry of the complex changes the probability of bond rupture [41]. Their experimental results for the repartition translational energy are 32% for the OD product and 25% when

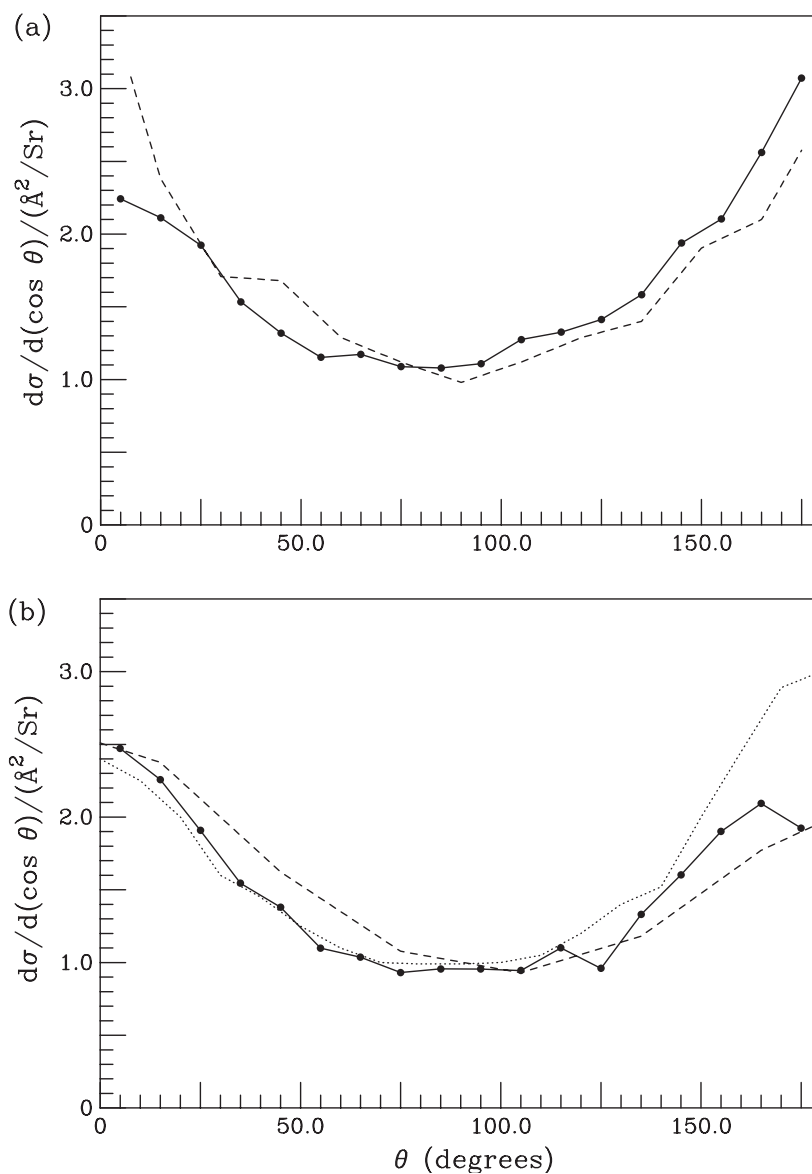


Figure 7. Differential cross sections for the reaction  $O(^1D) + D_2$  at collision energies of (a) 10.0 and (b) 22.2 kJ mol<sup>-1</sup>. Present work. (---) Experimental results (a) [1] and (b) [2]. (····) in (b) represents QCT results on the DK  $1^1A'$  PES [6].

Table 3. QCT results for the partition of the total kinetic energy into the translational, vibrational and rotational energy of the products for the reaction  $O(^1D) + H_2$ .

$E_{\text{col}}$ (kJ mol <sup>-1</sup> )	$E'_{\text{tr}}$ (%)	$E'_{\text{vib}}$ (%)	$E'_{\text{rot}}$ (%)
2.1	30.15	34.56	35.29
4.2	29.40	34.42	36.16
5.4	29.44	35.06	35.5
8.0	29.75	34.26	35.99
12.6	30.12	35.13	34.75
20.9	31.24	35.62	33.14

Table 4. QCT results for the partition of the total kinetic energy into the translational, vibrational and rotational energy of the products for the reaction  $O(^1D) + D_2$ .

$E_{\text{col}}$ (kJ mol <sup>-1</sup> )	$E'_{\text{tr}}$ (%)	$E'_{\text{vib}}$ (%)	$E'_{\text{rot}}$ (%)
2.1	30.34	33.45	36.21
4.2	29.32	33.73	36.95
10.0	30.52	33.73	35.75
20.9	30.84	35.41	33.75
22.2	31.29	35.30	33.41

Table 5. Phase space estimates of the partition of the total kinetic energy into the translational, vibrational and rotational energy of the products for the reaction  $O(^1D) + H_2$ .

$E_{\text{col}}$ (kJ mol <sup>-1</sup> )	$E'_{\text{tr}}$ (%)	$E'_{\text{vib}}$ (%)	$E'_{\text{rot}}$ (%)
2.1	36.83	41.12	22.06
4.2	36.74	39.97	23.28
5.4	36.71	39.60	23.69
8.0	36.76	38.67	24.53
12.6	37.30	37.56	25.14
20.9	38.42	36.10	25.48

considering the OH diatomic. These results are in close agreement with the 32.4 and 26.5% obtained from QCT calculations carried out at the same collision energy using the BR PES [61].

Similar plots for the same collisions are shown in figures 9 and 10 for vibrational and rotational product distributions. In figure 9, the obtained final QCT vibrational results are close to the associated Boltzmann distribution. However, with regard to the rotation distribution, figure 10 displays a noticeable divergence from the Boltzmann distribution, the quoted temperature of the fit being meaningless. The rotational distribution of the products peaks at higher  $N'$  values as

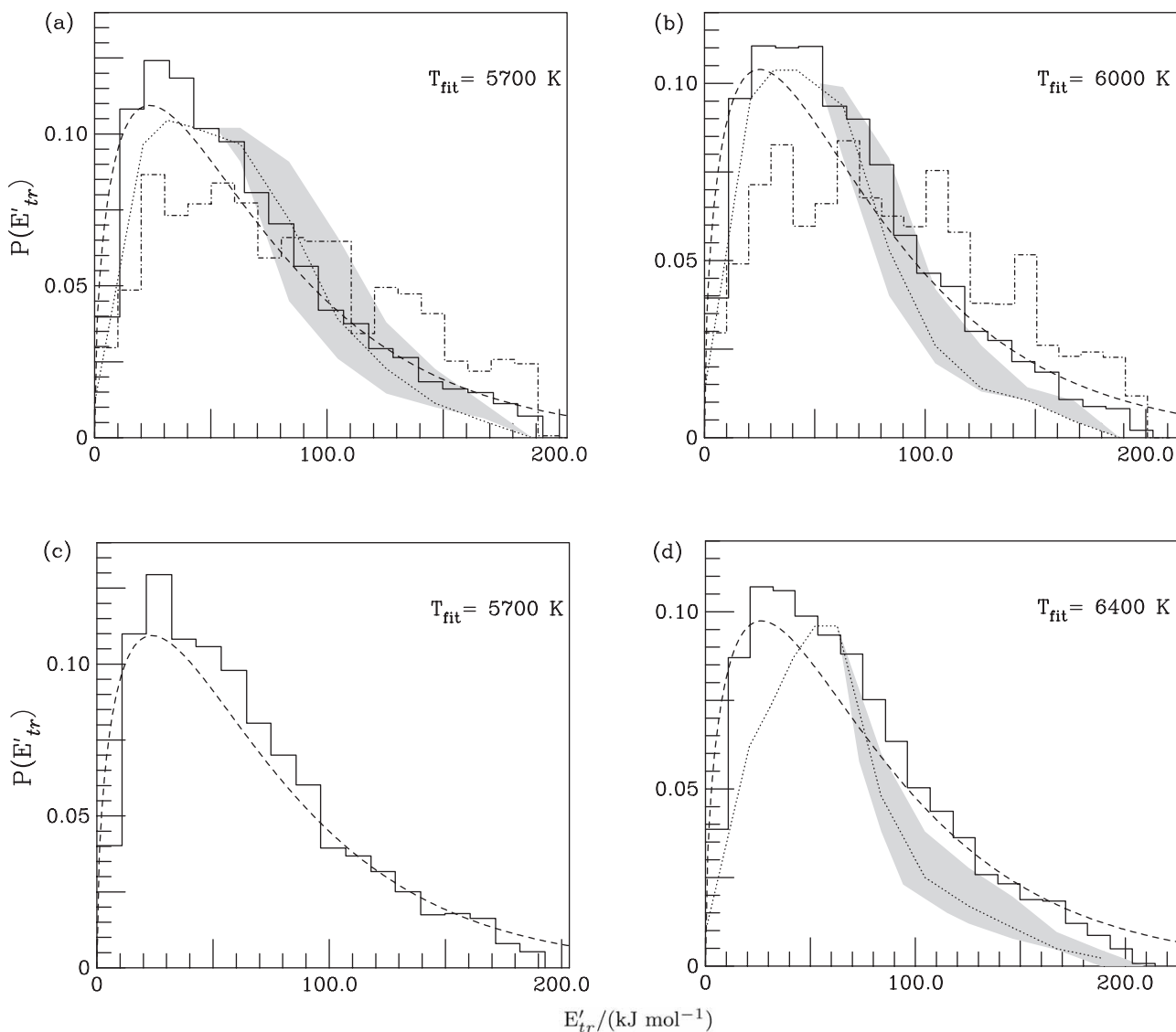


Figure 8. Translational energy distribution of the products obtained by the QCT method (—) and using statistical phase space calculations (- - - -). (· · · ·; shaded areas) The experimental results and respective error bars [2]. (- - - -) Coarse fit to a Maxwell-Boltzmann distribution;  $T_{\text{fit}}$  represents the associated temperature. (a, b) Reaction  $O(^1D) + H_2$  at collision energies of 8.0 and 12.6 kJ mol<sup>-1</sup>, respectively. (c, d) Reaction  $O(^1D) + D_2$  at collision energies of 10.0 and 22.2 kJ mol<sup>-1</sup>, respectively.

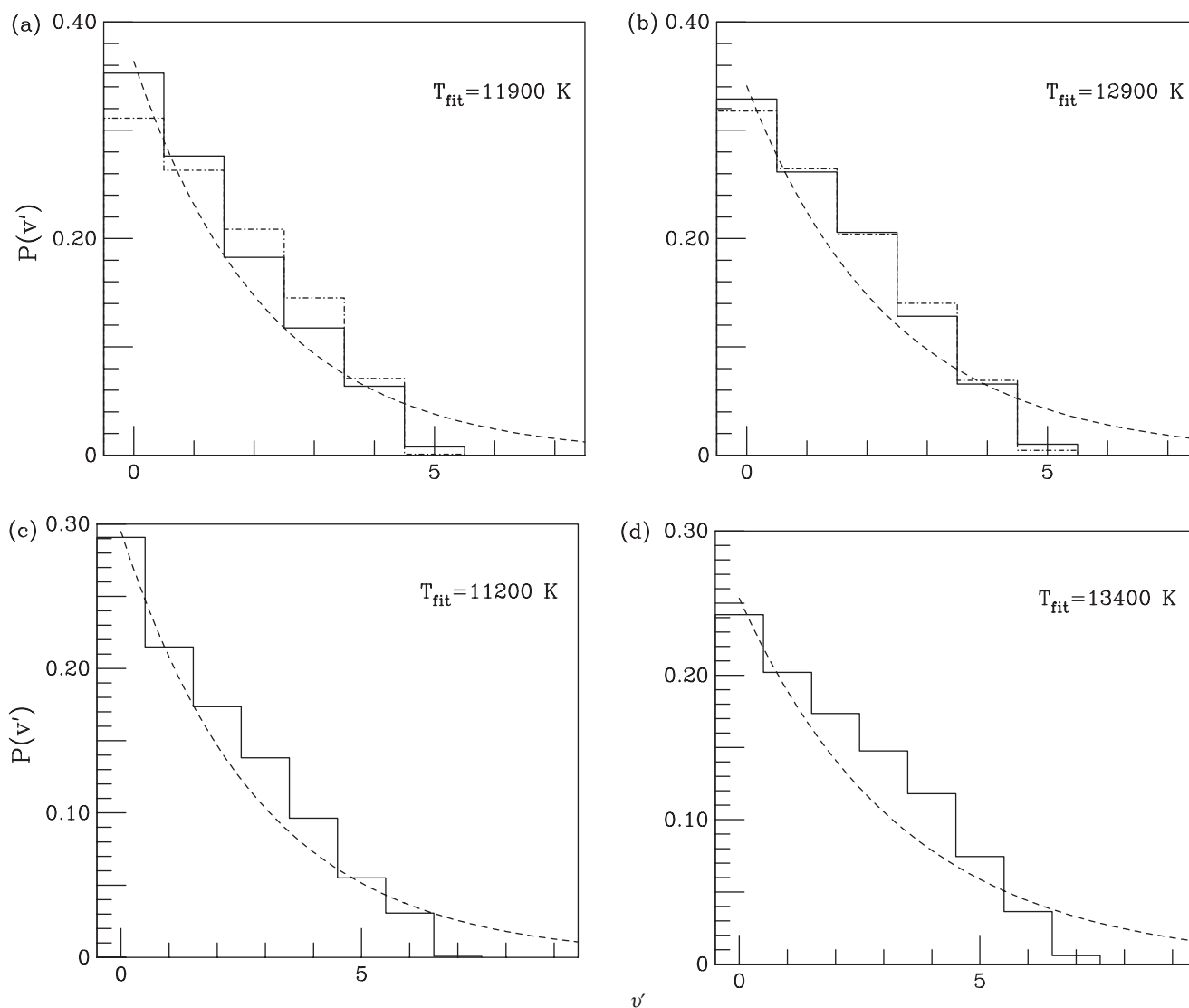


Figure 9. Vibrational distribution of the products. Plot descriptions as for figure 8.

a result of the insertion mechanism, in accordance with the experimental findings. Remember that the statistical prediction for the vibrational state of the products is similar to the trajectory results, whereas the statistical rotational distribution favours lower  $N'$  values, as noted previously.

A closer examination of these distributions should consider the rotational distribution for each vibrational level. Aoiz *et al.* [3, 4] published experimental results at an average collision energy of 0.12 eV (11.7 kJ mol<sup>-1</sup>). To make a comparison with those results we carried out quasiclassical trajectory calculations simulating the experimental conditions, as described in the work of Koppe *et al.* [62]. The latter authors presented the experimental rotational distributions of the OH

products for  $v' = 3$  and  $v' = 4$  and compared them with QCT and QM studies using the  $1^1A'$  and  $1^1A''$  surfaces. Those results (QCT and QM) were achieved using the K and DK PES and they concluded that the DK surfaces present a better description for the dynamics of the reaction  $O(^1D) + H_2$ .

As mentioned before, the reaction  $O(^1D) + H_2$  occurs predominantly through an insertion mechanism on the fundamental potential energy surface,  $1^1A'$ . For higher collision energies the excited states can also contribute to the reaction. On the first excited state,  $1^1A''$ , this reaction proceeds by an abstraction mechanism and populates, almost exclusively, the  $v' = 3$  and  $v' = 4$  levels of the product diatomic, OH. As the BR PES only describes the  $1^1A'$  ground state, in figure 11 we compare our results

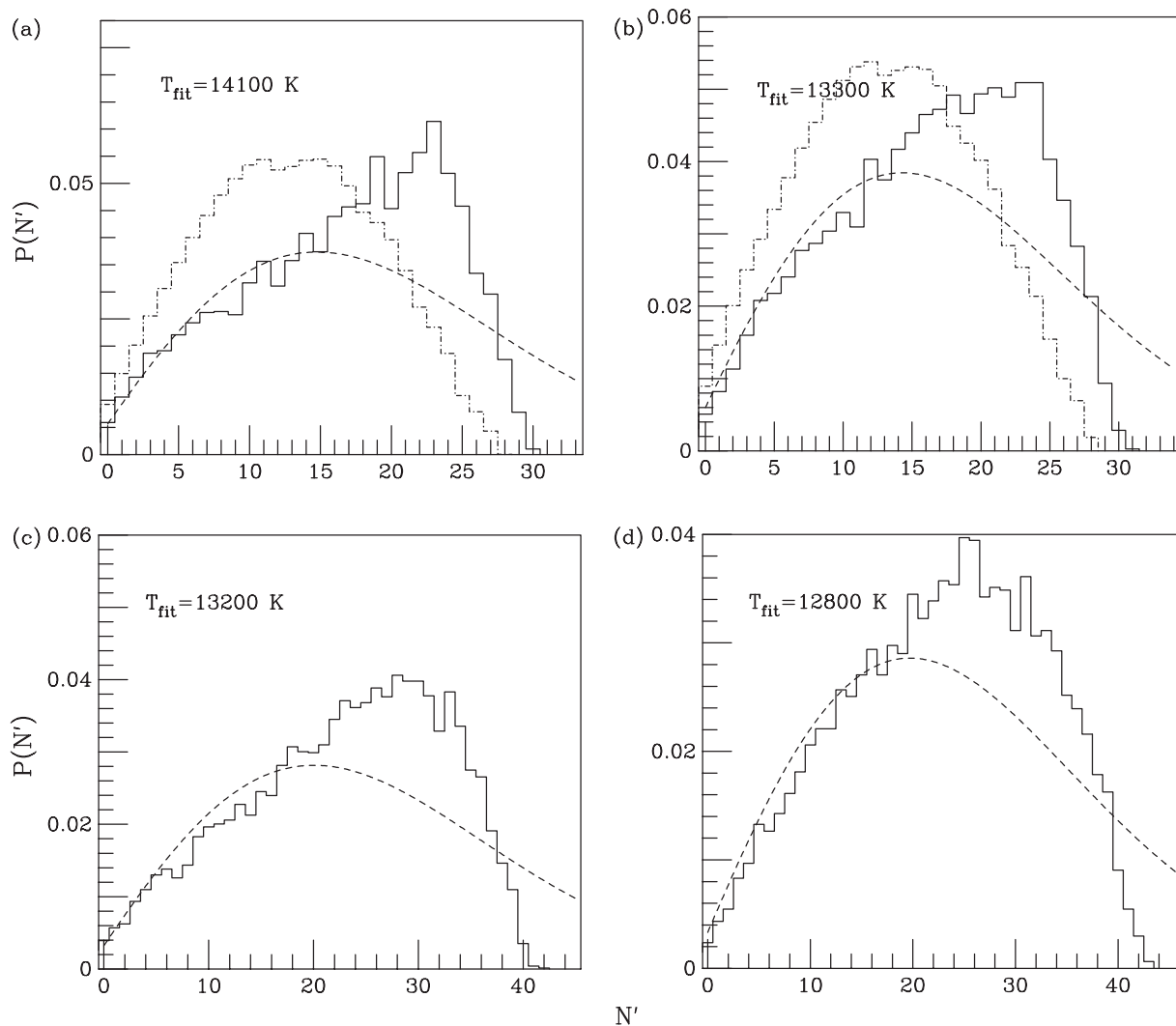


Figure 10. Rotational distribution of the products. Plot descriptions as for figure 8.

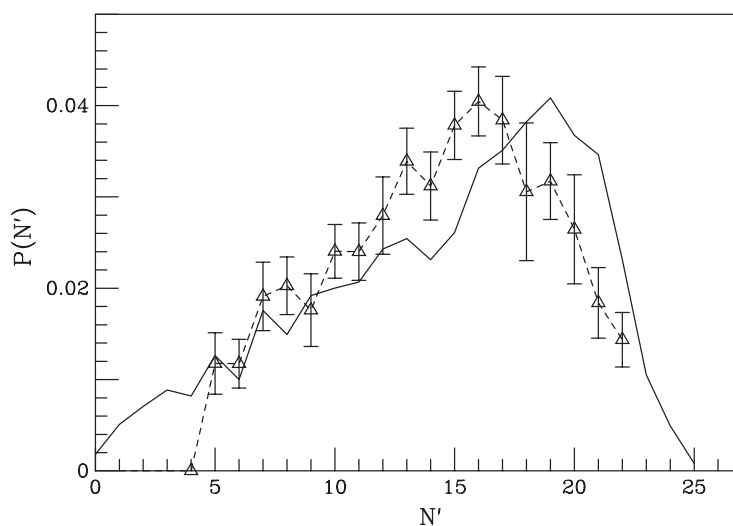


Figure 11. Distribution of the rotational population for the reaction  $\text{O}(^1\text{D}) + \text{H}_2$  for  $v' = 2$  at an average collision energy of  $11.7 \text{ kJ mol}^{-1}$ . ( $\Delta$ ; - - -) Experimental data [63]. (—) This work.

with the experimental rotational population for  $\nu' = 2$  [63], normalized for the sum of these three vibrational levels. In this figure,  $N'$  represents the diatomic rotational level and  $P(N')$  is the probability of finding the product at this level.

It should be pointed out that our results are obtained from classical calculations where the final attribution of vibrational and rotational quantum levels is a crude estimation. In addition, due to the orbital and spin angular moments of the  $^2\Pi$  state of the product OH diatomic, the definition of the nuclear rotational quantum number,  $N'$ , from the diatomic angular momentum is not a straightforward task. In this work, we started from the classical diatomic angular momentum to define an integer value for  $J'$ , as proposed [50], and we define the nuclear rotational quantum number using  $N' = J' - 1$ . A similar displacement of one between the classical and quantum results has been found in this system [5].

In percentile terms the experimental vibrational distribution gives 45.98, 33.20 and 20.82 for  $\nu' = 2$ ,  $\nu' = 3$  and  $\nu' = 4$ , respectively. We obtained 50.98, 32.52 and 16.50, in reasonable agreement with experiment, if we consider the contribution of the first excited state to the population of the  $\nu' = 3$  and  $\nu' = 4$  states. Considering only the ground-state surface, the QCT results give a value of 0.51 for the ratio  $P(\nu' = 4)/P(\nu' = 3)$ . This would appear to constitute a reasonable value compared with similar results obtained on the DK surface [3, 4], 0.47 (QCT) and 0.53 (QM), as shown in table 6.

Table 6. Relation  $P(\nu' = 4)/P(\nu' = 3)$ .

	BR PES QCT	DKPES [3, 4]		Exp. [3, 4]
		QCT	QM	
$1^1A'$ (only)	0.51	$0.47 \pm 0.01$	0.53	
$1^1A' + 1^1A''$		$0.60 \pm 0.01$	0.61	$0.59 \pm 0.05$

As far as we are aware, the most recent experimental study for the distribution of the rotational population for the reaction  $O(^1D) + H_2$  is [5]. These authors presented experimental results for the distribution of the rotational population at  $\nu' = 0, 1, 2, 3$  and 4 at a collision energy of 56 meV ( $5.4 \text{ kJ mol}^{-1}$ ), where the contribution of the excited states should be negligible. In figure 12, we compare our results with experiment. The agreement is very good.

## 5. Conclusion

The quasiclassical calculations we have performed using the BR PES [21] show good agreement with the experimental results. A global analysis of the angular distribution of the products for the studied reaction shows reasonable agreement between our results and the experimental data. Similar good agreement has been obtained for the energy distribution of the products. This would appear to confirm that the BR PES [21], based on high-quality *ab initio* data with a careful description of the long-range forces [11], correctly reproduces the main details of this system. However, as pointed out by Dunne and Murrell [64], because of the large exothermicity of the title reaction its outcome would not be greatly affected by inconsistencies in the exit channel, and the exchange reaction  $D + OH \rightarrow H + OD$  should also be considered.

The divergence observed between our results for quasiclassical trajectories and statistical predictions indicates that the details of the PES on the exit channel should play an important role, even for highly exothermic reactions with highly excited complexes where statistical theories should be valid.

The distribution of the rotational population of the OH product for different vibrational states has been analysed. Our results have been compared with

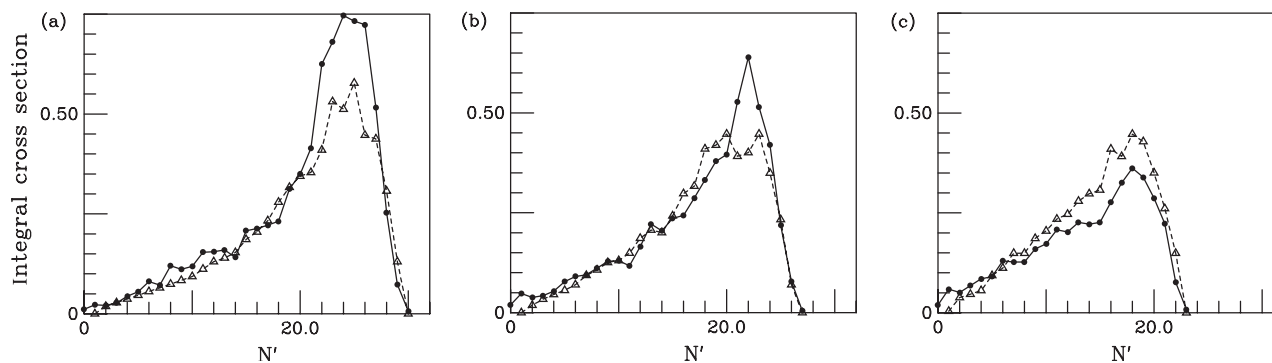


Figure 12. Experimental vs. QCT rotational integral cross sections (in  $\text{\AA}^2$ ) for the  $O(^1D) + H_2$  reaction at  $5.4 \text{ kJ mol}^{-1}$  collision energy for: (a)  $\nu' = 0$ , (b)  $\nu' = 1$  and (c)  $\nu' = 2$ . ( $\Delta$ ; - - -) Experimental data [5]. ( $\bullet$ ; —) This work.

experimental results [3–5, 63]. The comparison allows us to conclude that, even at the classical level, there is good agreement between theory and experiment.

## References

- [1] M. Ahmed, D. S. Peterka, and A. G. Suits, *Chem. Phys. Lett.* **301**, 372 (1999).
- [2] M. Alagia, N. Balucani, L. Cartechini, P. Casavecchia, E. H. van Kleef, G. G. Volpi, P. J. Kuntz, and J. J. Sloan, *J. Chem. Phys.* **108**, 6698 (1998).
- [3] F. J. Aoiz, L. Banares, M. Brouard, J. F. Castillo, K. Church, W. Denzer, P. Honvault, J. M. Launay, and C. Vallance, *Proceedings of the 13th European Conference on the Dynamics of Molecular Collisions (MOLEC 2000)*, Jerusalem, 2000.
- [4] F. J. Aoiz, L. Banares, J. F. Castillo, M. Brouard, W. Denzer, C. Vallance, P. Honvault, J.-M. Launay, A. J. Dobbyn, and P. J. Knowles, *Phys. Rev. Lett.* **86**, 1729 (2001).
- [5] F. J. Aoiz, L. Bañares, J. F. Castillo, V. J. Herrero, B. Martinez-Haya, P. Honvault, J.-M. Launay, X. Liu, J. J. Lin, S. A. Harich, C. C. Wang, and X. Yang, *J. Chem. Phys.* **116**, 10692 (2002).
- [6] N. Balucani, P. Casavecchia, F. J. Aoiz, L. Banares, J. F. Castillo, and V. J. Herrero, *Molec. Phys.* **103**, 1703 (2005).
- [7] Y.-T. Hsu, K. Liu, L. A. Pederson, and G. C. Schatz, *J. Chem. Phys.* **111**, 7921 (1999).
- [8] Y.-T. Hsu, K. Liu, L. A. Pederson, and G. C. Schatz, *J. Chem. Phys.* **111**, 7931 (1999).
- [9] M. H. Alexander, E. J. Rackam, and D. E. Manolopoulos, *J. Chem. Phys.* **121**, 5221 (2004).
- [10] F. J. Aoiz, L. Banares, J. F. Castillo, V. J. Herrero, and B. Martinez-Haya, *Phys. Chem. Chem. Phys.* **4**, 4379 (2002).
- [11] J. Brandão and C. M. A. Rio, *Chem. Phys. Lett.* **372**, 866 (2003).
- [12] R. J. Buss, P. Casavecchia, S. J. Sibener, and Y. T. Lee, *Chem. Phys. Lett.* **82**, 386 (1981).
- [13] K. Drukker and G. C. Schatz, *J. Chem. Phys.* **111**, 2451 (1999).
- [14] M. S. Fitzcharles and G. C. Schatz, *J. Phys. Chem.* **90**, 3634 (1986).
- [15] S. K. Gray, C. Petrongolo, K. Drukker, and G. C. Schatz, *J. Phys. Chem. A* **103**, 9448 (1999).
- [16] S. K. Gray, G. G. Balint-Kurti, G. C. Schatz, J. J. Lin, X. Liu, S. Harich, and X. Yang, *J. Chem. Phys.* **113**, 7330 (2000).
- [17] T.-S. Ho, T. Hollebeek, H. Rabitz, L. B. Harding, and G. C. Schatz, *J. Chem. Phys.* **105**, 10472 (1996).
- [18] T. Takayanagi, *J. Chem. Phys.* **116**, 2439 (2002).
- [19] A. J. C. Varandas, A. I. Voronin, A. Riganelli, and P. J. S. B. Caridade, *Chem. Phys. Lett.* **278**, 325 (1997).
- [20] A. J. C. Varandas, A. I. Voronin, P. J. S. B. Caridade, and A. Riganelli, *Chem. Phys. Lett.* **331**, 331 (2000).
- [21] J. Brandão and C. M. A. Rio, *J. Chem. Phys.* **119**, 3148 (2003).
- [22] A. J. Dobbyn and P. J. Knowles, *Molec. Phys.* **91**, 1107 (1997).
- [23] L. Halonen and T. Carrington, *J. Chem. Phys.* **88**, 4171 (1988).
- [24] P. Jensen, *J. Molec. Spectrosc.* **133**, 438 (1989).
- [25] E. Kauppi and L. Halonen, *J. Phys. Chem.* **94**, 5779 (1990).
- [26] J. N. Murrell, S. Carter, S. C. Farantos, P. Huxley, and A. J. C. Varandas, *Molecular Potential Energy Functions* (Chichester, Wiley, 1984).
- [27] O. Polyansky, P. Jensen, and J. Tennyson, *J. Chem. Phys.* **101**, 7651 (1994).
- [28] R. Schinke and W. A. Lester Jr, *J. Chem. Phys.* **72**, 3754 (1980).
- [29] A. J. C. Varandas, *J. Chem. Phys.* **105**, 3524 (1996).
- [30] A. J. C. Varandas, *J. Chem. Phys.* **107**, 867 (1997).
- [31] A. J. C. Varandas and A. I. Voronin, *Molec. Phys.* **85**, 497 (1995).
- [32] A. J. C. Varandas, A. I. Voronin, and P. J. S. B. Caridade, *J. Chem. Phys.* **108**, 7623 (1998).
- [33] T. E. Graedel and P. J. Crutzen, *Atmospheric Change—An Earth System Perspective* (W. H. Freeman, New York, 1993).
- [34] J. R. Barker, in *Progress and Problems in Atmospheric Chemistry*, edited by J. R. Barker (World Scientific, Singapore, 1995), p. 1.
- [35] J. W. Chamberlain and D. M. Hunten, *Theory of Planetary Atmospheres—An Introduction to Their Physics and Chemistry* (New York, Academic Press, 1987).
- [36] S. P. Sander, R. R. Friedl, A. R. Ravishankara, D. M. Golden, C. E. Kolb, M. J. Kurylo, M. J. Molina, G. K. Moortgat, H. Keller-Rudek, B. J. Finlayson-Pitts, P. H. Wine, R. E. Huie, and V. L. Orkin, *Chemical Kinetics and Photochemical Data for Use in Atmospheric Studies, JPL Publication 06-2* (NASA-Jet Propulsion Laboratory, Pasadena, California, 2006).
- [37] J. H. Seinfeld, in *Chemistry of Ozone in the Urban and Regional Atmosphere (Progress and Problems in Atmospheric Chemistry)*, edited by J. R. Barker (World Scientific, Singapore, 1995), p. 34.
- [38] M. Nicolet, *Adv. Chem. Phys.* **55**, 63 (1985).
- [39] H. S. Johnston, *A. Rev. Phys. Chem.* **26**, 315 (1975).
- [40] G. C. Schatz, A. Papaioannou, L. A. Pederson, L. B. Harding, T. Hollebeek, T.-S. Ho, and H. Rabitz, *J. Chem. Phys.* **107**, 2340 (1997).
- [41] D. C. Che and K. Liu, *J. Chem. Phys.* **103**, 5164 (1995).
- [42] H. Partridge and D. W. Schwenke, *J. Chem. Phys.* **106**, 4618 (1997).
- [43] F. Schneider, F. D. Giacomo, and F. A. Gianturco, *J. Chem. Phys.* **104**, 5153 (1996).
- [44] S. P. Walch and L. B. Harding, *J. Chem. Phys.* **88**, 7653 (1988).
- [45] J. Brandão and C. M. A. Rio, *Chem. Phys. Lett.* **377**, 523 (2003).
- [46] S. Y. Lin and H. Guo, *Chem. Phys. Lett.* **385**, 193 (2004).
- [47] W. Wang, E. Santos, and J. Brandão, *J. Chem. Phys.* **124**, 074305 (2006).
- [48] A. J. Dobbyn and P. J. Knowles, *Faraday Discuss.* **110**, 247 (1998).
- [49] J. T. Muckerman, *J. Chem. Phys.* **54**, 1155 (1971).
- [50] D. G. Truhlar and J. T. Muckerman, *Reactive scattering cross sections III. Quasiclassical and semiclassical methods, in Atom-Molecule Collision Theory*, edited by R. B. Bernstein (Plenum Press, New York, 1979), p. 505.
- [51] A. J. Alexander, F. J. Aoiz, L. Bañares, M. Brouard, V. J. Herrero, and J. P. Simons, *Chem. Phys. Lett.* **278**, 313 (1997).

- [52] R. K. Talukdar and A. R. Ravishankara, *Chem. Phys. Lett.* **253**, 177 (1996).
- [53] R. Altkinson, D. L. Baulch, R. A. Cox, R. F. Hampson Jr, J. A. Kerr, and J. Troe, *J. Phys. Chem. Ref. Data* **21**, 1125 (1992).
- [54] Y.-T. Hsu, J.-H. Wang, and K. Liu, *J. Chem. Phys.* **107**, 2351 (1997).
- [55] P. Honvault and J. M. Launay, *J. Chem. Phys.* **114**, 1057 (2001).
- [56] E. J. Rackham, T. Gonzalez-Lezana, and D. E. Manolopoulos, *J. Chem. Phys.* **119**, 12895 (2003).
- [57] J. N. Murrell and S. Carter, *J. Phys. Chem.* **88**, 4887 (1984).
- [58] P. Pechukas, J. C. Light, and C. Rankin, *J. Chem. Phys.* **44**, 794 (1966).
- [59] E. J. Rackham, F. Huarte-Larranaga, and D. E. Manolopoulos, *Chem. Phys. Lett.* **343**, 356 (2001).
- [60] F. J. Aoiz, L. Banares, M. Brouard, J. F. Castillo, and V. J. Herrero, *J. Chem. Phys.* **113**, 5339 (2000).
- [61] C. M. A. Rio and J. Brandão, *Chem. Phys. Lett.*, **433**, 268 (2007).
- [62] S. Koppe, T. Laurent, P. D. Naik, H.-R. Volpp, J. Wolfrum, T. Arusi-Parpar, I. Bar, and S. Rosenwaks, *Chem. Phys. Lett.* **214**, 546 (1993).
- [63] M. Brouard and C. Vallance, Personal communication.
- [64] L. J. Dunne and J. N. Murrell, *Molec. Phys.* **50**, 635 (1983).